Cell, Vol. 121, 703–712, June 3, 2005, Copyright ©2005 by Elsevier Inc. DOI 10.1016/j.cell.2005.03.023

The Cryo-EM Structure of a Translation Initiation Complex from *Escherichia coli*

Gregory S. Allen,[1] Andrey Zavialov,[2] Richard Gursky,[1] Måns Ehrenberg,[2] and Joachim Frank[1,3,*]
[1]Howard Hughes Medical Institute
Health Research, Inc. at the Wadsworth Center
Empire State Plaza
Albany, New York 12201
[2]Department of Cell and Molecular Biology
Biomedical Center
Box 596
S-751 24 Uppsala
Sweden
[3]Department of Biomedical Sciences
The State University of New York at Albany
Empire State Plaza
Albany, New York 12201

Summary

The 70S ribosome and its complement of factors required for initiation of translation in *E. coli* were purified separately and reassembled in vitro with GDPNP, producing a stable initiation complex (IC) stalled after 70S assembly. We have obtained a cryo-EM reconstruction of the IC showing IF2•GDPNP at the intersubunit cleft of the 70S ribosome. IF2•GDPNP contacts the 30S and 50S subunits as well as fMet-tRNA^{fMet}. IF2 here adopts a conformation radically different from that seen in the recent crystal structure of IF2. The C-terminal domain of IF2 binds to the single-stranded portion of fMet-tRNA^{fMet}, thereby forcing the tRNA into a novel orientation at the P site. The GTP binding domain of IF2 binds to the GTPase-associated center of the 50S subunit in a manner similar to EF-G and EF-Tu. Additionally, we present evidence for the localization of IF1, IF3, one C-terminal domain of L7/L12, and the N-terminal domain of IF2 in the initiation complex.

Introduction

Initiation of protein synthesis in eubacteria, during which the 50S and 30S ribosomal subunits are joined to form an elongation-competent 70S ribosome, requires a 30S preinitiation complex. In this preinitiation complex, the 30S subunit of the ribosome is associated with mRNA, initiator fMet-tRNA^{fMet}, and initiation factors 1 (IF1), 2 (IF2), and 3 (IF3) (Lockwood et al., 1971; Gualerzi and Pon, 1990). IF1 and IF2 have homologs in most organisms (Gualerzi and Pon, 1990; Lee et al., 1999), while IF3 lacks a eukaryotic homolog.

The Shine-Dalgarno sequence of mRNA, upstream of the AUG start codon, binds specifically to the 3′-terminal sequence of the 16S rRNA (Shine and Dalgarno, 1974). In this way, the mRNA becomes anchored to the 30S subunit, and the AUG start codon is positioned near the P site of the 30S subunit.

IF1 and IF3 are important for accelerating the rate of assembly of the preinitiation complex (Kay and Grunberg-Manago, 1972; Weiel and Hershey, 1982; Wintermeyer and Gualerzi, 1983; Pon and Gualerzi, 1984; Zucker and Hershey, 1986; Gualerzi and Pon, 1990), for prevention of initiation of protein synthesis with elongator tRNAs (Gualerzi et al., 1971; Canonaco et al., 1986; Hartz et al., 1989; Hartz et al., 1990; Gualerzi and Pon, 1990), and for formation of naked 70S ribosome complexes that lack tRNA in the P site (Grunberg-Manago et al., 1975). An important role for the G protein IF2 is to promote association of the ribosomal subunits (Grunberg-Manago et al., 1975) when an initiator tRNA is present on the 30S subunit (Lockwood et al., 1971; Antoun et al., 2003; Antoun et al., 2004). Although IF2 binds 30S subunits in the absence of GTP (Weiel and Hershey, 1982), rapid subunit association requires that IF2 be on the 30S subunit in the GTP form (Antoun et al., 2003; Antoun et al., 2004). The C terminus of IF2 recognizes both the 3′ single-stranded acceptor stem and the formylated methionine at the extreme 3′ end of fMet-tRNA^{fMet} (Guenneugues et al., 2000; Petersen et al., 1979; Petersen et al., 1981; Wakao et al., 1989). When IF2 binds to the 30S subunit together with initiator tRNA, its affinity to GTP is radically enhanced (Antoun et al., 2003), suggestive of cooperative binding of IF2 and fMet-tRNA^{fMet} to the 30S subunit (Groner and Revel, 1973; Wakao et al., 1990), and GTP binding is accompanied by a conformational change of IF2. Subsequent release of IF2 from the 70S initiation complex requires GTP hydrolysis on the factor (Grunberg-Manago et al., 1972; Luchin et al., 1999; Antoun et al., 2003; Antoun et al., 2004). The resulting 70S postinitiation complex (PIC) is the end product of initiation of protein synthesis in eubacteria.

While both X-ray and cryo-EM structures exist for two of the initiation factors bound to the 30S subunit, IF1•30S (Carter et al., 2001) and IF3•30S (McCutcheon et al., 1999; Pioletti et al., 2001), no structure of IF2 in complex with either the 30S subunit or the 70S ribosome has been reported. Roll-Mecak and coworkers solved the crystal structure of IF2 from *Methanobacterium thermoautotrophicum* bound to GTP; in this structure, the factor resembles a "chalice"; the N-terminal GTPase domain forms part of the cup portion of the chalice, while a long helix (H12) and the C-terminal fMet-tRNA^{fMet} binding domain form the stem and base, respectively (Roll-Mecak et al., 2000). Using various truncation mutants of IF2 in binding reactions with 30S or 50S subunits, which were then purified by pelleting of the resulting complex through a sucrose cushion, Moreno and coworkers delineated the specific domains of IF2 responsible for binding to the ribosomal subunits (Moreno et al., 1998; Moreno et al., 1999). Accordingly, the GTPase domain and domain III of IF2 interact with the 50S subunit, while portions of domain II, as well as the N-terminal domain of IF2, interact with the 30S subunit. Marzi and coauthors, using various nucleolytic

*Correspondence: joachim@wadsworth.org

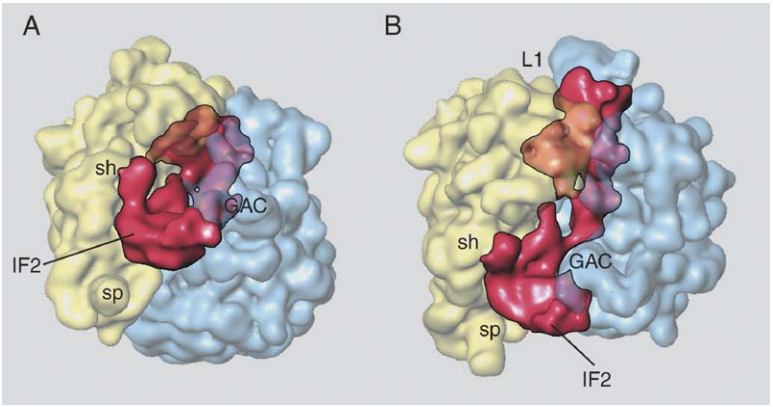

Figure 1. Cryo-EM Structure of the GDPNP-Stalled *E. coli* 70S Ribosome IC with IF2

The ligand density (red with black outline) was obtained by subtraction of the PIC density from the IC density.

(A) In this view, the N-terminal domains of IF2 are in the foreground. These interact with the 50S subunit (blue) at the GTPase-associated center (GAC) and with the 30S subunit (yellow) over a large surface on the intersubunit side of the shoulder (sh).

(B) The initiation complex has, with respect to (A), been rotated by ~45° around a horizontal axis and ~30° around the long axis of the ligand density. Additional labeled features also indicate the spur of the 30S (sp) subunit and the L1 stalk (L1).

reagents tethered to cysteines in IF2 from *Bacillus stearothermophilus*, demonstrated cleavages at specific sites on 16S and 23S rRNA from *Escherichia coli*. This information, in combination with the above-mentioned results, was used to model how IF2 binds to the 70S ribosome (Marzi et al., 2003).

We have formed a stable intermediate in the initiation pathway by substituting the nonhydrolyzable GTP analog GDPNP for GTP in our highly active in vitro system for protein synthesis (Zavialov et al., 2001). This ribosomal complex was obtained by mixing *E. coli* ribosomes with IF1, IF2, GDPNP, IF3, mRNA, and initiator tRNA. The rates of IF2-dependent subunit association with GTP and GDPNP are comparable (Antoun et al., 2003; Antoun et al., 2004). The conformation of IF2 in this complex provides the structural basis for our model of IF2-promoted association of subunits in the presence of initiator tRNA and GTP.

Our cryo-EM map of this stable intermediate shows IF2 in the intersubunit space, in contact with the 50S subunit, the 30S subunit, and initiator tRNA. The crystal structures of the GTP form of IF2 (PDB code 1G7T) and yeast $tRNA^{Phe}$ (PDB code 1EHZ), when fitted into the difference volume (i.e., IC – PIC), reveal the mutual interactions of these ligands and their contacts with the ribosome. However, our cryo-EM structure of IF2 within the 70S complex differs significantly from the crystal structure of free IF2 in its GTP form; cryo-EM in concert with X-ray crystallography can supply a more complete view of the relation between the structure and function of IF2 during initiation of protein synthesis.

Results

Reconstruction of the IC Volume

70S initiation complexes (ICs) with IF2 were formed in vitro for cryo-EM from individually prepared 70S *E. coli* ribosomes, IF1, IF2, IF3, fMet-$tRNA^{fMet}$, and mRNA together with the noncleavable GTP analog GDPNP. In the initial reconstruction from 55,270 particles, we made use of a previously determined cryo-EM reconstruction of the PIC containing mRNA and fMet-$tRNA^{fMet}$ in the P site (Valle et al., 2003a). Reconstruction and further refinement of the IC, using the PIC as a reference, yielded an 11.6 Å resolution (0.5 FSC) density map containing the 70S ribosome plus scattered densities, attributable to IF2, in the intersubunit space near the GTPase-associated center (GAC); the indistinctness of the mass suggested low occupancy of IF2 among the selected particles.

To circumvent this problem, we applied a method of supervised classification (Gao et al., 2004) to the same particle set, using reconstructions of the PIC and an EF-G bound 70S ribosome (Valle et al., 2003b) as alternative references. To reconstruct a density map of the IC with 100% IF2 occupancy, we computed the cross-correlation of each particle for both references and then selected that subset of particles with a higher crosscorrelation for the EF-G bound reference. This subset of particles was used in a reference-based alignment, with the EF-G bound 70S reconstruction as the initial reference. The resulting reconstruction of the IC was then iteratively refined to a resolution of 13.8 Å (0.5 FSC) (Supplemental Data) or 8.6 Å, as determined by the 3σ criterion. In this IC map, the ligand portion appears as a solid mass, with density comparable to that of the ribosomal proteins (Figure 1). We then fitted the coordinates of yeast $tRNA^{Phe}$ (Shi and Moore, 2000) and IF2 bound to GTP (see Experimental Procedures) into the ligand mass isolated from the new density map and refined the positions of these models as rigid bodies using RSRef (Chen et al., 2003; Gao et al., 2003; see Experimental Procedures).

Structural Model of IF2 in the IC

As an aid to interpretation of the IC volume, we isolated the ligand mass using the PIC as a guide (Figure 2). The shape of this mass was significantly different from the overall shape of the crystal structure of IF2•GTP (Figure 3). However, we found that straightforward changes in the relative orientations of the domains of IF2 could render its crystal form (Roll-Mecak et al., 2000; see Experimental Procedures) into a shape similar to its envelope in the difference map (Figure 2). Nevertheless, the portion of the map clearly attributable to the GTP binding domain (G domain) of IF2 is significantly larger than the G domain of the reoriented crystal structure. Therefore, to achieve an objective placement of the G domain within this region of the map, we applied a rapid motif-search algorithm (RAMOS/MOTIF in the SPIDER package; Rath et al., 2003) to the IC mass, using only the G domain coordinates of the crystal structure as a search motif. The highest peak found by the motif

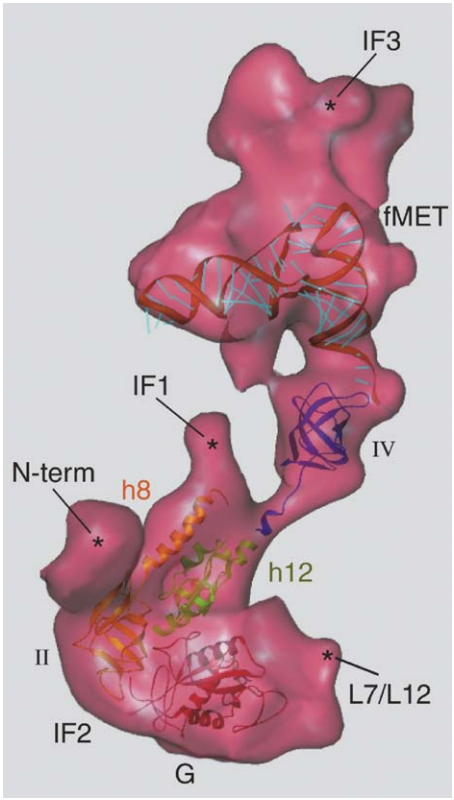

Figure 2. Interpretation of the IC-PIC Difference Map

The difference map is in approximately the same orientation as in Figure 1B. IF2 and fMet-tRNA^{fMet} (fMet) have been fitted to the cryo-EM density. Note that domain names and colors for this IF2 model follow the conventions of Roll-Mecak et al. (2000). Details of the interaction between IF2 domain IV and fMet-tRNA^{fMet} are apparent; our model suggests that domain IV of IF2 interacts only with single-stranded portions of the tRNA. The feature denoted N-term has no counterpart in the crystal structure of IF2: in the preparation of our sample we used the βIF2 protein, which contains an additional 150 amino acids N-terminal of the G domain. Density proximal to the C terminus of helix 8 (H8) of IF2 (domain II) is designated IF1, since this is the location of IF1 in the crystal structure (Carter et al., 2001). The difference density also may include a CTD of L7/L12 and IF3. Also note that domain III is not visible in this view.

search within this region of the map corresponded to a placement of the G domain of IF2 (Figure 2) in the same site on the ribosome as that occupied by the G domains of both ribosome bound EF-G (Figure 4A) and EF-Tu (Figure 4B) (Valle et al., 2003a). We found it striking that each G domain was independently fitted to different cryo-EM density maps yet they all concurred as to their placement and orientation relative to the 70S ribosome. The remainder of IF2 was fitted to the density as described in Experimental Procedures. We note that the resulting model of IF2 is in general agreement with the recently proposed model based on rRNA-cleavage footprinting data (Marzi et al., 2003).

One of the conformational changes in IF2 that we posit, based on comparison of the X-ray structure to our cryo-EM model, is a movement of helix H8 in domain II, which packs against the remainder of domain II and links it to domain III in the X-ray structure; movement of helix H8 is necessary and sufficient to fill a portion of the difference density map connecting the previously fitted domains II and III. At the C-terminal end of the reoriented helix H8 is a globular density in our map that we identify as IF1 for two reasons. First, binding studies have shown that IF1 interacts with domain II of IF2 (Moreno et al., 1999). Second, this placement of IF1 agrees with the factor's position in the crystal complex with the 30S subunit (see Experimental Procedures; Carter et al., 2001).

Figure 5 displays further details of the difference volume and its interactions with the ribosomal subunits. As expected, the G domain of IF2 contacts the 50S subunit in the vicinity of the GTPase-associated center (GAC) (Figure 5A); it approaches the 23S rRNA near bases 2650–2660 and protein L6 near residues 90–94. Domain II of IF2 covers a large area of the 30S subunit (Figure 5B), including 16S rRNA bases 55–58, 357–360, and 366–369. Domain III of IF2 interacts extensively with the surface of L14, while domain IV contacts a large surface of L16 as well as 23S rRNA bases 2550–2556 and 2601–2602. In all, IF2 renders inaccessible 3900 Å^2 of 70S surface area that was formerly solvent accessible: 2600 Å^2 on the 50S subunit and 1300 Å^2 on the 30S subunit (see Experimental Procedures).

30S Subunit Rotation

In Figure 6 we compare the 30S subunits from the IC and PIC density maps. When the two maps are superimposed so as to produce maximal crosscorrelation, their 50S subunit regions are virtually indistinguishable (not shown), with the exception of the head of the L1 stalk, while the 30S subunit portions of the 50S-aligned

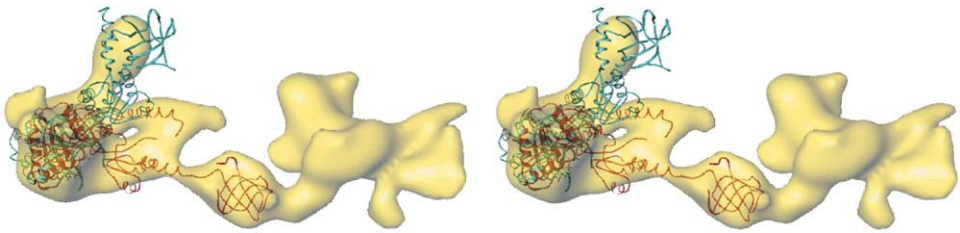

Figure 3. Stereoview Comparison of the Fit of Our IF2 model and the X-Ray Structure to the IC-PIC Difference Map

The crystal structure of IF2 from *M. thermoautotrophicum* (blue; PDB code 1G7T), with its G domain superimposed upon the G domain of our model of IF2 (red). The difference map to which our model was fitted is shown in yellow (see Figure 2). It is seen that our model of IF2 in the IC adopts a conformation quite different from the crystal structure of IF2.

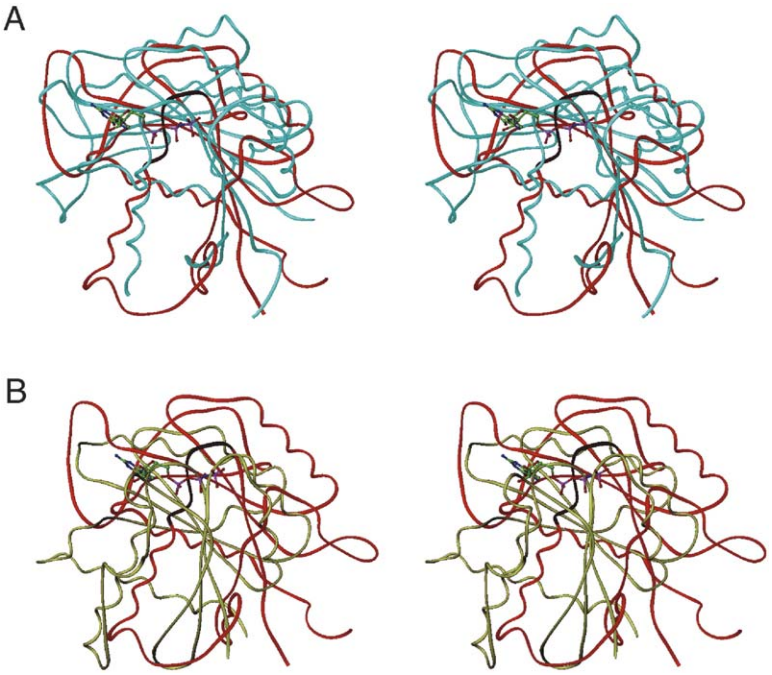

Figure 4. Stereoview Comparisons of G Domain Positions of IF2, EF-G, and EF-Tu

Each G domain was independently fitted to different cryo-EM density maps.
(A) EF-G (Valle et al., 2003b) versus IF2. G domains of EF-G and IF2 are blue and red, respectively. The GTP molecule is bound at the loop, between a strand and a helix, that defines the highly conserved P loop (black portion of IF2).
(B) EF-Tu (Valle et al., 2003b) versus IF2. G domains of EF-Tu and IF2 are green and red, respectively (the P loop of IF2 is colored black). The GTP model and the P loop illustrate the predicted orientation of, and binding-site location for, GTP on IF2's G domain in both panels; IF2 was brought into the same orientation in both panels.

maps differ significantly. The difference map shows a mass between the head of the L1 stalk and the fMet-tRNA (effectively occluding the E site) that may be partially due to motion of the stalk head but probably indicates the presence of another factor, the possible identity of which is discussed below. Evidently, the 30S subunit of the IC undergoes a general counterclockwise rotation (by ~4°) with respect to the 30S subunit of the PIC. The rotation is reminiscent of the conformational changes ("ratcheting") that were observed when EF-G•GDPNP was bound to the release complex in the presence of puromycin (Valle et al., 2003b), as well as changes seen earlier that were related to EF-G-mediated translocation (Frank and Agrawal, 2000).

Novel Hybrid P Site

Our placement of the C-terminal domain of IF2 in the IC volume sterically precludes classical P site binding of initiator tRNA (data not shown). To better compare the positions of the P site and P/E site tRNAs with the IC tRNA, we superimposed models of the three tRNAs on the basis of maximization of the correlation coefficient between the 30S portions of the relevant density maps (see Experimental Procedures); we found that the anticodon loops of all three maps superimpose. Remarkably, the IF2-fMet-tRNA^{fMet} interaction in the IC map exposes a novel site for initiator tRNA, intermediate between the classical P site and the P/E site, which we name the P/I site (i.e., P site on the 30S subunit, new position "I" on the 50S subunit) (Figure 7). Upon hydrolysis of GTP in the IC and subsequent dissociation of the bound initiation factors, the PIC is formed, with a classical P site fMet-tRNA^{fMet}. Clearly, then, the P/I site tRNA must move relative to the 30S subunit following hydrolysis of GTP. The motion required is a simple rotation in the plane of the tRNA by 20° about the anticodon loop; such a motion thereby translates the acyl moiety through a distance of 28 Å (Figure 7B).

Identification of Additional Factors and Domains

The ligand mass also reveals several regions of density not accounted for by the placement of IF2 and fMet-tRNA^{fMet} (Figure 2). One region of the density map for which the interpretation seems obvious lies near the G domain and domain II. This density extends across the surface of the 30S subunit toward the shoulder (sh) and interacts with 16S bases 37–38, 413–420, and 497–498. We assign this density to the N-terminal domain of *E. coli* βIF2, which does not exist in IF2 from *M. thermoautotrophicum* and therefore is absent from its crystal structure (Roll-Mecak et al., 2000). This location of the N-terminal domain of *E. coli* βIF2 agrees with crosslinking data for the complex of *B. stearothermophilus* IF2 with 16S rRNA, which demonstrated that the N-terminal domain of *B. stearothermophilus* IF2 is near guanine 423 of the 16S rRNA (Marzi et al., 2003); G423 of our 30S model is indeed within 20 Å of the density denoted N-term in Figure 2.

Another density region of unknown identity exists between the GAC and the G domain of IF2. Of course, our model includes L11 and other portions of the 50S subunit adjacent to the density in question, but these do not account for the unknown density. However, L7/L12 has been crosslinked to IF2 (Heimark et al., 1976), and the C-terminal domain (CTD) of L7/L12 has been strongly crosslinked to L11 (Dey et al., 1998). Furthermore, a cryo-EM structure of a 70S ribosome containing nanogold-labeled L7/L12 proteins showed the CTD to be next to L11 (Montesano-Roditis et al., 2001). Therefore, we suggest that the density in question is the CTD of L7/L12. Indeed, the recent NMR structure

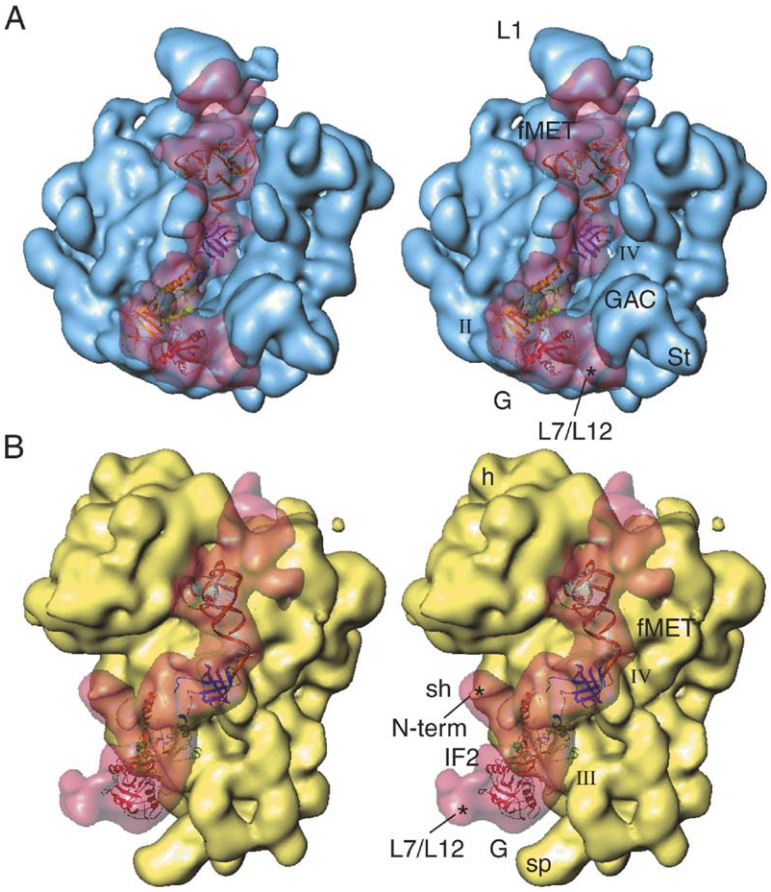

Figure 5. Difference Map-Ribosomal Subunit Contacts in the IC

(A) View of the IC-PIC difference map and its contacts with the intersubunit surface of the 50S subunit. With reference to Figure 1B, the 30S subunit has now been removed, and the 50S subunit has been rotated by ~90° around a vertical axis. St, stalk; L1, L1 stalk; G, II, and IV, G domain and domains II and IV of IF2; L7/L12, CTD of one monomer of L7/L12; N-term, N-terminal domain of βIF2; fMet, fMet-tRNA^{fMet}.

(B) View of the difference map and its interactions with the intersubunit surface of the 30S ribosomal subunit. With reference to Figure 1B, the 50S subunit has been removed, and the 30S subunit has been rotated by ~90° around a vertical axis. We clearly see the interaction of fMet-tRNA^{fMet} with domain IV of IF2. sh, shoulder; sp, spur; III, domain III of IF2.

of the CTD of L7/L12 (Bocharov et al., 2004) fits the density well, as shown in Figure S3.

Even when these tentative assignments have been made, a region of difference density remains unidentified—specifically, density on the side of the initiator tRNA distal to IF2 (Figure 2). Due to its proximity to the E site, we attempted to fit a tRNA to this unassigned density, but without success. However, we noticed that the difference density is strikingly similar in position and shape to a recent model of IF3 bound to the 30S subunit (Dallas and Noller, 2001), and we have therefore tentatively fitted this region of density with the atomic structures of IF3 (Figure S3).

Discussion

We successfully reconstituted the *E. coli* 70S initiation complex, stalled by GDPNP, using separately purified factors and ribosomes. Translation assays performed in parallel with complex assembly and using components from the same lots of purified factors and ribosomes gave high activity (data not shown). Therefore, we are confident that the cryo-EM structure of the stalled *E. coli* 70S initiation complex that we report here represents the true solution structure of the complex. As expected, IF2 and fMet-tRNA^{fMet} were located in the intersubunit space. Owing to the interaction with IF2, fMet-tRNA^{fMet} is forced into a novel hybrid P site on the 30S subunit. We have also located the N-terminal domain of *E. coli* IF2 in the long "thumb" of density extending across the surface of the 30S subunit in our map of the IC.

We also found that IF2 buries 2600 Å^2 of the 50S subunit's surface area. Burial of surfaces of comparable size commonly occurs at dimerization interfaces; indeed, IF2's role as the catalyst of 50S subunit association is analogous to that of a partner in dimerization. A survey of published binding affinities for dimerization interactions shows that such interactions have a high ΔG (<–10 kcal/mole), which corresponds to binding affinities on the order of K_D ~ nM or better (Brooijmans et al., 2002). Therefore, we hypothesize that the burial of IF2 surface area probably accounts for the mechanism of subunit association as well as the relatively high stability of the 70S intermediate containing IF2•GDPNP, here called the IC (Antoun et al., 2003; Antoun et al., 2004).

The observation that IF2's affinity for GTP on the 30S subunit is greatly enhanced by the presence of initiator tRNA suggests the occurrence of a GTP-dependent conformational change of the factor; this change is a prerequisite for rapid subunit association (Antoun et al., 2003; Antoun et al., 2004). Furthermore, the GDP and GTP forms of IF2 in the crystal are significantly different from one another, suggesting that GTP hydrolysis on IF2 in the 70S initiation intermediate reduces the area of the IF2•50S subunit interface, which in turn leads to decreased affinity and rapid dissociation of the factor.

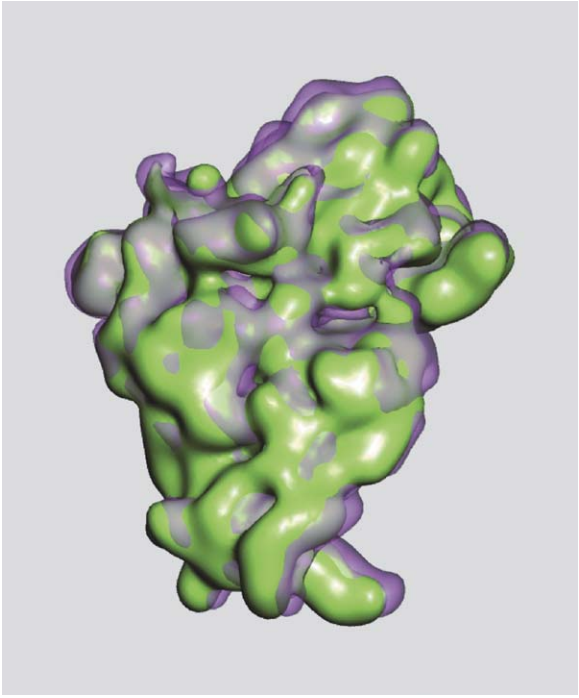

Figure 6. Rotation of the 30S Ribosomal Subunit between the IC and PIC Complexes

The IC and PIC (Valle et al., 2003b) maps were filtered at 13.8 Å and aligned with respect to their 50S subunits only. The 30S subunit from the PIC is green, while that from the IC is violet. Most of the differences between the two complete ribosome density maps appear in the 30S subunit region. There is a general counterclockwise rotation of the 30S subunit in the IC by ~4° with respect to the 30S subunit in the PIC.

In the absence of a structure for the 30S preinitiation complex, it is not known whether the conformations of IF2 and fMet-tRNA^{fMet} change upon association of the 50S subunit followed by 70S formation. It is clear, however, that GTP hydrolysis on IF2 in the 70S IC must result in a structural rearrangement of the ribosome to allow for fMet-tRNA^{fMet} movement into the classic P/P site. Since IF2 recognizes structural elements of the initiator tRNA, it could provide an accuracy step in initiation, ensuring that the IC is formed with only initiator tRNA (Huang et al., 1997; Shin et al., 2002). If all noninitiator tRNAs bind to IF2, albeit at a much lower affinity than does the initiator tRNA (Mayer et al., 2003), and if any tRNA can occupy the P site, a means for excluding noninitiator tRNAs must exist. We suggest that a higher standard free energy exists for any tRNA at the P/I site than for that tRNA at the P site; this increase in standard free energy raises the energy barrier too high for elongator tRNAs, which would already be destabilized by the noncognate interaction with the AUG start codon. Accordingly, P/I site binding and formation of the 70S IC could be strongly inhibited for elongator tRNAs but could be allowed for fMet-tRNA^{fMet}. Thus, the IC with IF2 in the GTP form may provide a checkpoint at which initiation can be aborted when the cognate initiator tRNA has been substituted by an elongator tRNA. Abortion may be effected either by redissociation of ribosomal subunits or else by dissociation of the elongator tRNA from the IC, followed by recycling of the 70S ribosome (minus tRNA) by the action of the RRF and EF-G (Karimi et al., 1999).

It is clear from the results of our placement of the G domain of IF2, using the motif search on the IC volume, that the G domains of EF-Tu, EF-G, and IF2 all occupy the same site on the ribosome, in roughly equivalent orientations (Figure 3). Furthermore, although these G domains have significant differences in both sequence

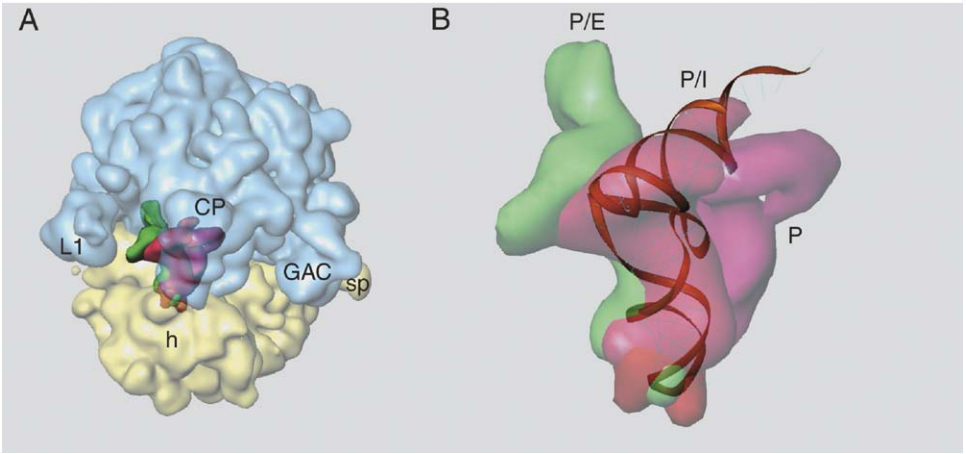

Figure 7. Comparison of tRNA in the P/I Site of the Initiation Complex with Its P Site and P/E Site Positions

(A) This view of the IC density map optimally shows the various P site tRNAs. The P site on the 30S subunit (yellow) is visible due to transparent rendering of both subunits (50S subunit in blue); the central protuberance (CP) is the chief structure here. Canonical P site (purple); P/E hybrid site (green); P/I site discovered in this work (red); h, head; sp, spur; L1, L1 stalk; GAC, GTPase center.

(B) Close-up of the P site tRNA variants. In going from the P site to the P/I site, the initiator tRNA rotates by ~20° about an axis through the anticodon, normal to the plane of the page; its acyl moiety moves by about 28 Å. By comparison, the P-to-P/E transition involves a rotation of ~35° about the long axis of the tRNA, as well as a rotation of ~35° about an axis through the anticodon, normal to the plane of the page; in this case, the acyl moiety moves by about 68 Å.

and structure, the number of features that they have in common is striking (Roll-Mecak et al., 2000). These observations suggest that there exists a general mechanism by which the ribosome effects GTP hydrolysis on these factors. However general this mechanism might be for the ribosome, it probably does not conform to the canonical GTPase mechanism, which normally involves intrusion of activity partners into the GTP binding pocket so as to provide a conserved side chain, such as lysine or arginine, that is directly involved in hydrolysis (Vetter and Wittinghofer, 2001). Yet, in the case of the ribosome-factor interactions noted above, there are no ribosomal protein residues proximal to the binding site of the factors. The factor's P loop, which is the site of GTP binding, could only interact with the sarcin-ricin loop (SRL) of the 23S rRNA, approximately 8 Å distant. Thus, the SRL has been identified as the GTPase-activating factor (Blanchard et al., 2004). Possibly the phosphate backbone of the SRL coordinates a metal ion, which could foster hydrolysis (Beaudry et al., 1979). However, previous structural and crosslinking data, taken together with our data, suggest that the C-terminal domain of L7/L12 intercalates between L11 and the G domain of IF2. Additionally, L7/L12 is known to be required for rapid hydrolysis of GTP on EF-Tu and EF-G (Mohr et al., 2002). Therefore, we suggest that the L7/L12 C-terminal domain induces conformational changes in the G domain, and these changes then stimulate the GTPase activity of IF2 (Mohr et al., 2002; Bocharov et al., 2004).

We have previously shown that ribosome-dependent GTP hydrolysis on ribosome release factor RF3 and EF-G requires a deacylated tRNA in the P site (Zavialov and Ehrenberg, 2003), allowing for the tRNA's movement into a hybrid P/E site (Valle et al., 2003b). When a noninitiator tRNA occupies the P site, the same is true for IF2; i.e., there is strong GTP hydrolysis when the tRNA is deacylated, but not otherwise. In contrast, when the P site is occupied by fMet-tRNA^{fMet}, there is strong idling GTPase activity by IF2 (Zavialov and Ehrenberg, 2003). The explanation for this behavior, we suggest, is that GTP hydrolysis on RF3, EF-G, and IF2 requires that, in each case, the CCA end of the P site tRNA move toward the E site. When the P site tRNA lacks peptide, this is easily achieved through hybrid P/E site binding of the tRNA. When the P site tRNA has a peptide, movement of the tRNA's CCA end toward the E site is effectively prevented by a high standard free-energy barrier so that the GTPase activity of all three factors is inhibited. It is only when the P site tRNA is fMet-tRNA^{fMet} that IF2 in the GTP form, with its strong affinities for both the initiator tRNA and the 50S subunit, can drive the ribosome into the intermediate IC, in which hydrolysis of IF2 is induced. This interpretation lends strong support to the above-suggested accuracy function of the IC: if an aminoacyl tRNA rather than an initiator tRNA is present in the preinitiation complex, then the IC cannot be formed, and initiation will be aborted.

Finally, we propose that IF3 is present in the IC. However, the authors who initially proposed the manner in which IF3 binds to the 30S subunit point out that their model predicts a clash between the C-terminal domain of IF3 and helix 69 of the 50S subunit (Dallas and Noller, 2001). We note that helix 69 is visible in both the IC map and the PIC map. When the two density maps are aligned so as to maximize the crosscorrelation, both helices 69 overlay precisely—that is, helix 69 does not move at all. Also, in the PIC map, helix 69 contacts fMet-tRNA, which is in the P site, but in the IC map, fMet-tRNA has been pushed out of the P site by IF2, thus making space between helix 69 and fMet. The space created between helix 69 and fMet also corresponds to a mass of density in the difference map (Figure S3); the volume associated with the mass in the difference map is approximately the right size for the C-terminal domain (CTD) of IF3. Biochemical data (Gualerzi and Pon, 1990; Pon and Gualerzi, 1986) suggest that 70S ribosome formation from the 50S subunit and a preinitiation 30S complex requires either that IF3 leave the 30S subunit before the 50S subunit can associate or else that IF3 dissociate from the 70S ribosome as a result of subunit association. In either scenario, there should therefore be no IF3 in the 70S initiation complex. It is, however, possible that IF3 is released from the 70S ribosome upon hydrolysis of GTP on IF2, in which case the presence of IF3 in the IC with IF2•GDPNP would be consistent with the second scenario of Gualerzi and collaborators (Gualerzi and Pon, 1990). Indeed, results of recent experiments using kinetic techniques suggest that IF3 remains in the IC complex until P_i is released (Grigoriadou et al., 2004). Early experiments (Goss et al., 1982) also suggested that 70S ribosomes can complex with IF3. Our present results lead us to conclude that IF3 is present in the IC (GDPNP).

Experimental Procedures

Preparation of Initiation Complexes

For preparation of the complex, a 300 μl mixture containing 2.7 μM *E. coli* ribosomes, 6.7 μM *E. coli* IF1, 6.7 μM *E. coli* β form of IF2 (Nyengaard et al., 1991), 4 μM *E. coli* IF3, 8.1 μM mRNA encoding for MFTI tetrapeptide (Zavialov et al., 2001), 7.6 μM *E. coli* fMet-tRNA^{fMet}, and 0.6 mM GDPNP was incubated at 37°C for 25 min. Then the mixture was diluted to 1 μM ribosome concentration with 0.5 mM GDPNP and 2 μM IF1, and it was aliquoted and frozen with liquid nitrogen. Prior to the cryo-EM analysis, an aliquot containing the complex was further diluted to 32 nM ribosome concentration with a dilution mixture containing 4 μM IF1, 2 μM βIF2, and 0.5 mM GDPNP. The incorporation of [^{3}H]fMet-tRNA^{fMet} into the initiation complex detected by nitrocellulose filtration was greater than 75%. Translation assays performed in parallel with the purified initiation complex, using βIF2, IF1, and GDPNP, showed that the initiated ribosome is nearly saturated with βIF2•GDPNP (Zavialov and Ehrenberg, 2003).

Cryo-EM and Image Processing

Thin carbon was floated onto Quantifoil grids (Quantifoil Micro Tools GMBH, Jena, Germany). A 5 μl aliquot was placed on each grid. The grids were then blotted, plunge frozen in liquid ethane, and stored in liquid nitrogen until data collection. Data were collected on a Tecnai F20 (FEI Company, Hillsboro, Oregon) at 200 kV and a magnification of 50,000 (±2%), under low-dose conditions. Micrographs were scanned at 14 μm resolution, giving 2.82 Å per pixel. One hundred and fourteen micrographs were each assigned to one of 21 defocus groups ranging from 0.93 to 3.93 μm underfocus. Particles (55,270) could easily be identified on the micrographs as 70S ribosomes. Each of the 70S particle images was initially aligned by crosscorrelation to 83 equispaced projections of a 3D reference, here the PIC, yielding the particle orientation as a set of Eulerian angles. The aligned particle images were backprojected

to yield a 3D reconstruction of the IC. Alignment and orientation parameters of the particles were iteratively refined with decreasing angular increments using standard methods. The SPIDER/WEB suite of programs (Frank et al., 1996) was used for all image processing. The resolution was estimated by a Fourier shell correlation cutoff of 0.5 to be 11.6 Å.

At this point it was clear that a significant number of the particles were 70S ribosomes from which one or more of the factors had dissociated. A method of supervised classification, also implemented in SPIDER, was used to separate images according to ligand occupancy. In this method, each image is compared with two reference density maps, here the PIC and an EF-G bound 70S ribosome (Valle et al., 2003b), and is then assigned to one of two classes, depending on the size of its crosscorrelation coefficient with respect to the two references (Gao et al., 2004). Figure S1 shows a histogram plot of the difference between the crosscorrelation values of each image with respect to both references; the class of images having a larger crosscorrelation coefficient with respect to the EF-G bound ribosome (particles plotted to left of zero, i.e., ligand bound form) was then used to reconstruct the IC volume. The initial image set contained 55,270 particles, which supervised classification pared to 20,283 particles for the IC volume. Following supervised classification, the resolution was estimated by a Fourier shell correlation cutoff of 0.5 to be 13.8 Å and by the 3σ criterion to be 8.6 Å.

Docking and Modeling of IF2, IF1, and P/I Site tRNA

The ModPipe server provided an excellent *E. coli* IF2 model (Pieper et al., 2004) based on the X-ray crystal structure of IF2 from *M. thermoautotrophicum* (PDB code 1G7T, Roll-Mecak et al., 2000). Since the region of the IC map corresponding to the G domain probably contains density for other molecules and domains (i.e., L7/L12 and domain III), we initially placed the G domain of IF2 using the rapid motif-search procedure implemented in SPIDER (Rath et al., 2003). The IC density map was searched systematically for crosscorrelation maxima using a 3D volume constructed from the coordinates of the G domain. Using the visualization program O (Jones et al., 1991), domain II was placed into the difference density using the location of the G domain and the crystal-structure conformation of IF2 as a reference (Roll-Mecak et al., 2000). Additionally, the cleavage patterns of rRNA by two mutant IF2s with tethered nucleases in domain II provided further constraints on the conformation of domain II (Marzi et al., 2003). Domain III could only be fitted by eye since no constraints were available and since the apparent conformation would necessitate large movements from the crystal-structure form. However, helix 12 was easily recognizable in the final refined density map. As helix 12 connects domain III with domain IV, a domain which is globular and interacts with fMet-tRNA^{fMet}, we found it straightforward to fit domain IV and the initiator tRNA. To improve the fit to the IC map, the hand-fitted models of IF2 and fMet-tRNA^{fMet} were subjected to rigid-body refinement using a real-space refinement program (RSRef, Gao et al., 2003). To calculate the surface area buried by IF2, the software suite CNS was applied using a 1.4 Å probe radius (Brunger et al., 1998).

We fitted the IF1 model by overlaying the IF1:30S crystal-structure model (Carter et al., 2001) on the 30S subunit coordinates obtained by RSRef applied to the IC map; the resulting IF1 model nicely filled the extra EM density found at the end of helix 8 of our model of IF2. Note that the domain numbering (i.e., G–IV) follows the crystal-structure convention (Roll-Mecak et al., 2000), whereas the residue numbering adheres to the βIF2 sequence (i.e., the first residue of the crystal structure is residue 224 of βIF2).

The P site tRNAs were superimposed on the basis of the translational shifts that maximized the crosscorrelation of the respective 30S subunits with which they were associated. In order to superimpose the three fMet-tRNAs, as in Figure 7, we performed real-space refinement with the coordinates of the P site tRNA from Valle and coworkers (Valle et al., 2003a). As expected, this procedure brought all three anticodons into virtually perfect alignment.

The models were manipulated by hand in O (Jones et al., 1991). Figures were prepared in RIBBONS (Carson, 1997) and IRIS Explorer 5.

Supplemental Data

Supplemental Data include three figures and are available with this article online at http://www.cell.com/cgi/content/full/121/5/703/DC1/.

Acknowledgments

We thank Michael Watters for assistance with the illustrations, and we thank Adriana Verschoor, Jayati Sengupta, Ayman Antoun, and Michael Pavlov for comments on the manuscript. This work was supported by HHMI and NIH grants R37 GM29169 and R01 GM 55440 (J.F.) and by the Swedish Research Council and the Swedish Foundation for Strategic Research (M.E.).

Received: December 21, 2004
Revised: March 14, 2005
Accepted: March 22, 2005
Published: June 2, 2005

References

Antoun, A., Pavlov, M.Y., Andersson, K., Tenson, T., and Ehrenberg, M. (2003). The roles of initiation factor 2 and guanosine triphosphate in initiation of protein synthesis. EMBO J. *22*, 5593–5601.

Antoun, A., Pavlov, M.Y., Tenson, T., and Ehrenberg, M.M. (2004). Ribosome formation from subunits studied by stopped-flow and Rayleigh light scattering. Biol. Proced. Online *6*, 35–54.

Beaudry, P., Sander, G., Grunberg-Manago, M., and Douzou, P. (1979). Cation-induced regulatory mechanism of GTPase activity dependent on polypeptide initiation factor 2. Biochemistry *18*, 202–207.

Blanchard, S.C., Gonzalez, R.L., Kim, H.D., Chu, S., and Puglisi, J.D. (2004). tRNA selection and kinetic proofreading in translation. Nat. Struct. Mol. Biol. *11*, 1008–1014.

Bocharov, E.V., Sobol, A.G., Pavlov, K.V., Korzhnev, D.M., Jaravine, V.A., Gudkov, A.T., and Arseniev, A.S. (2004). From structure and dynamics of protein L7/L12 to molecular switching in ribosome. J. Biol. Chem. *279*, 17697–17706.

Brooijmans, N., Sharp, K.A., and Kuntz, I.D. (2002). Stability of macromolecular complexes. Proteins *48*, 645–653.

Brunger, A.T., Adams, P.D., Clore, G.M., DeLano, W.L., Gros, P., Grosse-Kunstleve, R.W., Jiang, J.S., Kuszewski, J., Nilges, M., Pannu, N.S., et al. (1998). Crystallography & NMR system: A new software suite for macromolecular structure determination. Acta Crystallogr. D Biol. Crystallogr. *54*, 905–921.

Canonaco, M.A., Calogero, R.A., and Gualerzi, C.O. (1986). Mechanism of translational initiation in prokaryotes. Evidence for a direct effect of IF2 on the activity of the 30 S ribosomal subunit. FEBS Lett. *207*, 198–204.

Carson, M. (1997). Ribbons. Methods Enzymol. *277*, 493–505.

Carter, A.P., Clemons, W.M., Jr., Brodersen, D.E., Morgan-Warren, R.J., Hartsch, T., Wimberly, B.T., and Ramakrishnan, V. (2001). Crystal structure of an initiation factor bound to the 30S ribosomal subunit. Science *291*, 498–501.

Chen, J.Z., Furst, J., Chapman, M.S., and Grigorieff, N. (2003). Low-resolution structure refinement in electron microscopy. J. Struct. Biol. *144*, 144–151.

Dallas, A., and Noller, H.F. (2001). Interaction of translation initiation factor 3 with the 30S ribosomal subunit. Mol. Cell *8*, 855–864.

Dey, D., Bochkariov, D.E., Jokhadze, G.G., and Traut, R.R. (1998). Cross-linking of selected residues in the N- and C-terminal domains of Escherichia coli protein L7/L12 to other ribosomal proteins and the effect of elongation factor Tu. J. Biol. Chem. *273*, 1670–1676.

Frank, J., and Agrawal, R.K. (2000). A ratchet-like inter-subunit reorganization of the ribosome during translocation. Nature *406*, 318–322.

Frank, J., Radermacher, M., Penczek, P., Zhu, J., Li, Y., Ladjadj, M., and Leith, A. (1996). SPIDER and WEB: processing and visualiza-

tion of images in 3D electron microscopy and related fields. J. Struct. Biol. *116*, 190–199.

Gao, H., Sengupta, J., Valle, M., Korostelev, A., Eswar, N., Stagg, S.M., Van Roey, P., Agrawal, R.K., Harvey, S.C., Sali, A., et al. (2003). Study of the structural dynamics of the E coli 70S ribosome using real-space refinement. Cell *113*, 789–801.

Gao, H., Valle, M., Ehrenberg, M., and Frank, J. (2004). Dynamics of EF-G interaction with the ribosome explored by classification of a heterogeneous cryo-EM dataset. J. Struct. Biol. *147*, 283–290.

Goss, D.J., Parkhurst, L.J., and Wahba, A.J. (1982). Kinetic studies on the interaction of chain initiation factor 3 with 70 S Escherichia coli ribosomes and subunits. J. Biol. Chem. *257*, 10119–10127.

Grigoriadou, C., Marzi, S., Seo, H.S., Dongli, P., Kirillov, S., Gualerzi, C.O., and Cooperman, B.S. (2004). IF2, IF3 and thiostrepton interaction during initiation complex formation. In Translational Control, A. Hinnebusch, T. Pestova, and J. Richter, eds. (Cold Spring Harbor, New York: Cold Spring Harbor Laboratory Press), pp. 407.

Groner, Y., and Revel, M. (1973). Escherichia coli initiation factors: isolation of an IF2-fMet-transfer RNA complex. J. Mol. Biol. *74*, 407–410.

Grunberg-Manago, M., Dondon, J., and Graffe, M. (1972). Inhibition by thiostrepton of the IF-2-dependent ribosomal GTPase. FEBS Lett. *22*, 217–221.

Grunberg-Manago, M., Dessen, P., Pantaloni, D., Godefroy-Colburn, T., Wolfe, A.D., and Dondon, J. (1975). Light-scattering studies showing the effect of initiation factors on the reversible dissociation of Escherichia coli ribosomes. J. Mol. Biol. *94*, 461–478.

Gualerzi, C., Pon, C.L., and Kaji, A. (1971). Initiation factor dependent release of aminoacyl-tRNAs from complexes of 30S ribosomal subunits, synthetic polynucleotide and aminoacyl tRNA. Biochem. Biophys. Res. Commun. *45*, 1312–1319.

Gualerzi, C.O., and Pon, C.L. (1990). Initiation of mRNA translation in prokaryotes. Biochemistry *29*, 5881–5889.

Guenneugues, M., Caserta, E., Brandi, L., Spurio, R., Meunier, S., Pon, C.L., Boelens, R., and Gualerzi, C.O. (2000). Mapping the fMet-tRNA(f)(Met) binding site of initiation factor IF2. EMBO J. *19*, 5233–5240.

Hartz, D., McPheeters, D.S., and Gold, L. (1989). Selection of the initiator tRNA by Escherichia coli initiation factors. Genes Dev. *3*, 1899–1912.

Hartz, D., Binkley, J., Hollingsworth, T., and Gold, L. (1990). Domains of initiator tRNA and initiation codon crucial for initiator tRNA selection by Escherichia coli IF3. Genes Dev. *4*, 1790–1800.

Heimark, R.L., Hersehy, J.W., and Traut, R.R. (1976). Cross-linking of initiation factor IF2 to proteins L7/L12 in 70 S ribosomes of Escherichia coli. J. Biol. Chem. *251*, 779–784.

Huang, H.K., Yoon, H., Hannig, E.M., and Donahue, T.F. (1997). GTP hydrolysis controls stringent selection of the AUG start codon during translation initiation in Saccharomyces cerevisiae. Genes Dev. *11*, 2396–2413.

Jones, T.A., Zou, J.Y., and Cowan, S.W. (1991). Improved methods for building protein models in electron density maps and the location of errors in these models. Acta Crystallogr. A *47*, 110–119.

Karimi, R., Pavlov, M.Y., Buckingham, R.H., and Ehrenberg, M. (1999). Novel roles for classical factors at the interface between translation termination and initiation. Mol. Cell *3*, 601–609.

Kay, A.C., and Grunberg-Manago, M. (1972). The mechanism of action of initiation factor IF1: non-analogy with elongation factor EFTs. Biochim. Biophys. Acta *277*, 225–230.

Lee, J.H., Choi, S.K., Roll-Mecak, A., Burley, S.K., and Dever, T.E. (1999). Universal conservation in translation initiation revealed by human and archaeal homologs of bacterial translation initiation factor IF2. Proc. Natl. Acad. Sci. USA *96*, 4342–4347.

Lockwood, A.H., Chakraborty, P.R., and Maitra, U. (1971). A complex between initiation factor IF2, guanosine triphosphate, and fMet-tRNA: an intermediate in initiation complex formation. Proc. Natl. Acad. Sci. USA *68*, 3122–3126.

Luchin, S., Putzer, H., Hershey, J.W., Cenatiempo, Y., Grunberg-Manago, M., and Laalami, S. (1999). In vitro study of two dominant inhibitory GTPase mutants of Escherichia coli translation initiation factor IF2. Direct evidence that GTP hydrolysis is necessary for factor recycling. J. Biol. Chem. *274*, 6074–6079.

Marzi, S., Knight, W., Brandi, L., Caserta, E., Soboleva, N., Hill, W.E., Gualerzi, C.O., and Lodmell, J.S. (2003). Ribosomal localization of translation initiation factor IF2. RNA *9*, 958–969.

Mayer, C., Kohrer, C., Kenny, E., Prusko, C., and RajBhandary, U.L. (2003). Anticodon sequence mutants of Escherichia coli initiator tRNA: effects of overproduction of aminoacyl-tRNA synthetases, methionyl-tRNA formyltransferase, and initiation factor 2 on activity in initiation. Biochemistry *42*, 4787–4799.

McCutcheon, J.P., Agrawal, R.K., Philips, S.M., Grassucci, R.A., Gerchman, S.E., Clemons, W.M., Jr., Ramakrishnan, V., and Frank, J. (1999). Location of translational initiation factor IF3 on the small ribosomal subunit. Proc. Natl. Acad. Sci. USA *96*, 4301–4306.

Mohr, D., Wintermeyer, W., and Rodnina, M.V. (2002). GTPase activation of elongation factors Tu and G on the ribosome. Biochemistry *41*, 12520–12528.

Montesano-Roditis, L., Glitz, D.G., Traut, R.R., and Stewart, P.L. (2001). Cryo-electron microscopic localization of protein L7/L12 within the Escherichia coli 70 S ribosome by difference mapping and Nanogold labeling. J. Biol. Chem. *276*, 14117–14123.

Moreno, J.M., Kildsgaard, J., Siwanowicz, I., Mortensen, K.K., and Sperling-Petersen, H.U. (1998). Binding of *Escherichia coli* initiation factor IF2 to 30S ribosomal subunits: a functional role for the N-terminus of the factor. Biochem. Biophys. Res. Commun. *252*, 465–471.

Moreno, J.M., Drskjotersen, L., Kristensen, J.E., Mortensen, K.K., and Sperling-Petersen, H.U. (1999). Characterization of the domains of E. coli initiation factor IF2 responsible for recognition of the ribosome. FEBS Lett. *455*, 130–134.

Nyengaard, N.R., Mortensen, K.K., Lassen, S.F., Hershey, J.W., and Sperling-Petersen, H.U. (1991). Tandem translation of E. coli initiation factor IF2 beta: purification and characterization in vitro of two active forms. Biochem. Biophys. Res. Commun. *181*, 1572–1579.

Petersen, H.U., Roll, T., Grunberg-Manago, M., and Clark, B.F. (1979). Specific interaction of initiation factor IF2 of E. coli with formylmethionyl-tRNA f Met. Biochem. Biophys. Res. Commun. *91*, 1068–1074.

Petersen, H.U., Kruse, T.A., Worm-Leonhard, H., Siboska, G.E., Clark, B.F., Boutorin, A.S., Remy, P., Ebel, J.P., Dondon, J., and Grunberg-Manago, M. (1981). Study of the interaction of Escherichia coli initiation factor IF2 with formylmethionyl-tRNAMetf by partial digestion with cobra venom ribonuclease. FEBS Lett. *128*, 161–165.

Pieper, U., Eswar, N., Braberg, H., Madhusudhan, M.S., Davis, F.P., Stuart, A.C., Mirkovic, N., Rossi, A., Marti-Renom, M.A., Fiser, A., et al. (2004). MODBASE, a database of annotated comparative protein structure models, and associated resources. Nucleic Acids Res. *32* (Database issue), D217–D222.

Pioletti, M., Schlunzen, F., Harms, J., Zarivach, R., Gluhmann, M., Avila, H., Bashan, A., Bartels, H., Auerbach, T., Jacobi, C., et al. (2001). Crystal structures of complexes of the small ribosomal subunit with tetracycline, edeine and IF3. EMBO J. *20*, 1829–1839.

Pon, C.L., and Gualerzi, C.O. (1984). Mechanism of protein biosynthesis in prokaryotic cells. Effect of initiation factor IF1 on the initial rate of 30 S initiation complex formation. FEBS Lett. *175*, 203–207.

Pon, C.L., and Gualerzi, C.O. (1986). Mechanism of translational initiation in prokaryotes. IF3 is released from ribosomes during and not before 70 S initiation complex formation. FEBS Lett. *195*, 215–219.

Rath, B.K., Hegerl, R., Leith, A., Shaikh, T.R., Wagenknecht, T., and Frank, J. (2003). Fast 3D motif search of EM density maps using a locally normalized cross-correlation function. J. Struct. Biol. *144*, 95–103.

Roll-Mecak, A., Cao, C., Dever, T.E., and Burley, S.K. (2000). X-Ray structures of the universal translation initiation factor IF2/eIF5B: conformational changes on GDP and GTP binding. Cell *103*, 781–792.

Shi, H., and Moore, P.B. (2000). The crystal structure of yeast phenylalanine tRNA at 1.93 A resolution: a classic structure revisited. RNA *6*, 1091–1105.

Shin, B.S., Maag, D., Roll-Mecak, A., Arefin, M.S., Burley, S.K., Lorsch, J.R., and Dever, T.E. (2002). Uncoupling of initiation factor eIF5B/IF2 GTPase and translational activities by mutations that lower ribosome affinity. Cell *111*, 1015–1025.

Shine, J., and Dalgarno, L. (1974). The 3′-terminal sequence of Escherichia coli 16S ribosomal RNA: complementarity to nonsense triplets and ribosome binding sites. Proc. Natl. Acad. Sci. USA *71*, 1342–1346.

Valle, M., Zavialov, A., Li, W., Stagg, S.M., Sengupta, J., Nielsen, R.C., Nissen, P., Harvey, S.C., Ehrenberg, M., and Frank, J. (2003a). Incorporation of aminoacyl-tRNA into the ribosome as seen by cryo-electron microscopy. Nat. Struct. Biol. *10*, 899–906.

Valle, M., Zavialov, A., Sengupta, J., Rawat, U., Ehrenberg, M., and Frank, J. (2003b). Locking and unlocking of ribosomal motions. Cell *114*, 123–134.

Vetter, I.R., and Wittinghofer, A. (2001). The guanine nucleotide-binding switch in three dimensions. Science *294*, 1299–1304.

Wakao, H., Romby, P., Westhof, E., Laalami, S., Grunberg-Manago, M., Ebel, J.P., Ehresmann, C., and Ehresmann, B. (1989). The solution structure of the Escherichia coli initiator tRNA and its interactions with initiation factor 2 and the ribosomal 30 S subunit. J. Biol. Chem. *264*, 20363–20371.

Wakao, H., Romby, P., Laalami, S., Ebel, J.P., Ehresmann, C., and Ehresmann, B. (1990). Binding of initiation factor 2 and initiator tRNA to the Escherichia coli 30S ribosomal subunit induces allosteric transitions in 16S rRNA. Biochemistry *29*, 8144–8151.

Weiel, J., and Hershey, J.W. (1982). The binding of fluorescein-labeled protein synthesis initiation factor 2 to Escherichia coli 30 S ribosomal subunits determined by fluorescence polarization. J. Biol. Chem. *257*, 1215–1220.

Wintermeyer, W., and Gualerzi, C. (1983). Effect of Escherichia coli initiation factors on the kinetics of N-Acphe-tRNAPhe binding to 30S ribosomal subunits. A fluorescence stopped-flow study. Biochemistry *22*, 690–694.

Zavialov, A.V., and Ehrenberg, M. (2003). Peptidyl-tRNA regulates the GTPase activity of translation factors. Cell *114*, 113–122.

Zavialov, A.V., Buckingham, R.H., and Ehrenberg, M. (2001). A post-termination ribosomal complex is the guanine nucleotide exchange factor for peptide release factor RF3. Cell *107*, 115–124.

Zucker, F.H., and Hershey, J.W. (1986). Binding of Escherichia coli protein synthesis initiation factor IF1 to 30S ribosomal subunits measured by fluorescence polarization. Biochemistry *25*, 3682–3690.

Accession Numbers

The cryo-EM maps have been deposited in the 3D-EM database, EMBL-European Bioinformatics Institute, Cambridge: EMD-3523 (70S·IF2·GDPNP·IF1·IF3·mRNA·fMet-tRNA^{fMet} initiation complex) and EMD-3666 (IC-PIC difference map). Atomic models have been deposited in the Protein Data Bank under the following ID codes: IZ01 (IF2·GDPNP, IF1, and tRNA fitted to the IC map) and IZ03 (P site and P/E site tRNA used for comparison with P/I).